Modeling of Non-Isothermal Film Blowing Process for Non-Newtonian Fluids by Using Variational Principles

Modified on Friday, 01 May 2015 10:21 PM by mpieler — Categorized as: Paper of the Month

Modeling of Non-Isothermal Film Blowing Process for Non-Newtonian Fluids by Using Variational Principles

Martin Zatloukal[1,2], Roman Kolarik[1,2]

[1] Polymer Centre, Faculty of Technology, Tomas Bata University in Zlín, nám. T. G. Masaryka 275, 762 72 Zlín, Czech Republic

[2] Centre of Polymer Systems, Tomas Bata University in Zlín, nám. T. G. Masaryka 5555, 760 01 Zlín, Czech Republic

Abstract

In this work, non-isothermal film blowing process analysis for non-Newtonian polymer melts has been performed theoretically by using minimum energy approach and the obtained predictions were compared with both, theoretical and experimental data (internal bubble pressure, take-up force, bubble shape, velocity and temperature profiles) taken from the open literature. For this purpose, recently proposed generalized Newtonian fluid depending on three principal invariants of the deformation rate tensor, D, and its absolute defined as (square-root of D*D) has been used. It has been found that film blowing model predictions are in very good agreement with the corresponding experimental data.

Introduction

The film blowing process is an important polymer processing operation which is widely used for thin polymer films production [1-29]. These biaxially oriented films of a small thickness are used in commodity applications, such as food wrapping and carrier bags in food processing, medical films, scientific balloons, garbage bags and waste land fill liners in the waste industry. The relationships between the machine design, processing parameters, material and the extensional stresses within the extending bubble are still not fully understood although they have been investigated by many researchers from the late 1930´s [1-14]. The most popular way to optimize the film blowing process is modeling. The first film blowing model was developed by Pearson and Petrie [20, 22] for isothermal process and Newtonian fluid where the film is assumed to be a thin shell in tension in the axial and circumferential directions. This model became the basis of the most subsequent film blowing models [15-17, 24, 26, 30-36]. However, numerical instabilities [26, 29], inability to describe the full range of the bubble shapes [27] and existence of anomalous predictions [37-38] were identified in the open literature if one tried to solve the Pearson-Petrie equations with particular constitutive equations. It has been recently found that these problems can be overcome by the use of the Zatloukal-Vlcek model [30-36] which describes the formation of the bubble, due to the internal bubble pressure and the take-up force, in such a way that the resulting bubble satisfies the minimum energy requirements.

The main aim in this work is to investigate predicting capabilities of the Zatloukal-Vlcek model if nonisothermal conditions and non-Newtonian fluid behavior are taken into account. The studied model behavior will be compared with Tas's PhD thesis experimental data [18] and predictions of the following two different Pearson and Petrie based models: Sarafrazi and Sharif model [16] (eXtended Pom-Pom constitutive equation is used; a variable heat transfer coefficient and stress induced crystallization is taken into account and Beaulne and Mitsoulis model [15] (integral constitutive equation of the K-BKZ type is utilized; constant heat transfer coefficient and no crystallization effects are assumed).

Mathematical modeling

Zatloukal-Vlcek model

The Zatloukal-Vlcek model is based on the assumption that bubble during blowing can be viewed as a elastic membrane (characterized by the one constant value of compliance J where the thickness is neglected) which is bended due to the internal load, p, and take-up force, F in such a way, that bubble shape satisfies minimum energy requirements [34]. Under these assumptions, the model yields analytical expressions for bubble shape, take-up force and internal bubble pressure which are summarized in Table 1. The model is given by the following four physical parameters: freezeline height, L, bubble curvature, pJ (which is given by the bubble compliance, J, and the internal load, p), the blow-up ratio, BUR, and the die radius, R_0. The function, which occurs in both equations for bubble shape and take-up force, depends on parameter A according to Table 2. Just note that in Eq. 1 in Table 1, y represents the bubble radius at particular distance from the die exit x (x=0 at the die exit; x=L at the freezeline height).

Non-isothermal film blowing with non-Newtonian fluid

Continuity equation:

$$Q = 2\pi y(x)h(x)v(x) \tag{1}$$

where Q is the volume flow rate, y(x), the radius of the bubble, h(x), the thickness of the film and v(x) is the film velocity, all as functions of the distance from the die x. Secondly,

$$\tau = 2\eta\left(I_{|D|}, II_D, III_D\right)D \tag{2}$$

where means the extra stress tensor, D represents the deformation rate tensor and stands for the viscosity, which is not constant (as in the case of standard Newtonian law), but it is allowed to vary with the first invariant of the absolute value of deformation rate tensor

$I_{|D|} = tr(|D|)$, (where $|D|$ is defined as the square root of D^2) as well as on the second $II_D = 2tr(D^2)$, and third, $III_D = det(D)$, invariants of D according to Eq. 3

$$\eta\left(I_{|D|}, II_D, III_D\right) = \eta(II_D)^{f\left(I_{|D|}, II_D, III_D\right)} \tag{3}$$

where $\eta(II_D)$ is given by the well known Carreau-Yasuda model, Eq. 4 and $f\left(I_{|D|}, II_D, III_D\right)$ is given by Eq. 5,.

$$\eta(II_D) = \frac{\eta_0 a_T}{\left[1 + \left(\lambda a_T \sqrt{II_D}\right)^a\right]^{\left(\frac{1-n}{a}\right)}} \tag{4}$$

$$f\left(I_{|D|}, II_D, III_D\right) = \left\{ tanh\left[\alpha a_T\left(1 + \frac{1}{4\left(\sqrt{3}\right)^3}\right)^{-\psi}\left(1 + \frac{III_D}{II_D^{3/2}}\right)^\psi \frac{\sqrt[3]{4|III_D|} + I_{|D|}}{3} + \beta\right]\frac{1}{tanh(\beta)}\right\}^\varsigma \tag{5}$$

Here η_0, λ, a, n, α, ψ, β, ς are adjustable parameters and a_T is temperature shift factor defined by the Arrhenius equation:

$$a_T = exp\left[\frac{E_a}{R}\left(\frac{1}{273.15+T} - \frac{1}{273.15+T_r}\right)\right] \tag{6}$$

where E_a is the activation energy, R is the universal gas constant, T_r is the reference temperature and T is local bubble temperature. It is not difficult to show that the equation of continuity together with the generalized Newtonian model yields the following expression for the internal force at the freezeline in the machine direction:

$$F_N = 2\overline{\overline{\eta}}\,\overline{\dot{\varepsilon}_1}\frac{Q}{v_f} \tag{7}$$

where $\overline{\eta}$ and $\overline{\dot{\varepsilon}_1}$ represent the mean values of the melt viscosity $\left(\overline{\eta} = \frac{1}{L}\int_0^L \eta\, dx\right)$ and the extensional rate $\left(\overline{\dot{\varepsilon}_1} = \frac{1}{L}\int_0^L \dot{\varepsilon}\, dx\right)$, respectively, for the whole bubble, Q, the volume flow rate, v_f, the velocity of the film at the freezeline. The equation for bubble compliance J can be obtained by solving Eqs. 4 in Table 1, $F_{total} = |F|$ and Eq. 7 in the following form:

$$J = \frac{L^2 v_f}{2\varphi\overline{\overline{\eta}}\,\overline{\dot{\varepsilon}_1}Q} \tag{8}$$

Energy Equation: With the aim to take non-isothermal conditions into account, cross-sectionally averaged energy equation taken from [40], has been considered:

$$\rho C_p \frac{dT}{dx} = -\frac{2\pi y \rho}{\dot{m}}\left[HTC(T-T_{air}) + \sigma_B \bar{\varepsilon}\left(T^4 - T_{air}^4\right)\right] + \tau : \nabla v + \rho \Delta H_f \frac{d\phi}{dx} \quad (9)$$

where Cp stands for the specific heat capacity, ρ is the polymer density, y means the local bubble radius, m is the mass flow rate, HTC represents the heat transfer coefficient, T is the bubble temperature, T_{air} means the air temperature used for the bubble cooling, σ_B stands for the Stefan-Boltzmann constant, ε represents the emissivity, τ is the extra stress tensor, (upsidedown delta)v means velocity gradient tensor, ΔH_f indicates the heat of crystallization per unit mass and Φ is the average absolute crystallinity degree of the system at the axial position, x.

In order to reduce the problem complexity, the axial conduction, dissipation, radiation effects and crystallization are neglected. For such simplifying assumptions, the Eq. 9 is reduced in the following, the simplest version of the cross-sectionally averaged energy equation:

$$\dot{m} C_p \frac{dT}{dx} = 2\pi y \left[HTC(T-T_{air})\right] \quad (10)$$

where the local bubble radius y is given by Eq. 1 in Table 1. The Eq. 10 applied for the whole part of the bubble takes the following form:

$$\int_{T_{die}}^{T_{solid}} \frac{\dot{m} C_p}{HTC(T-T_{air})} dT = 2\pi \int_{0}^{\bar{L}} y dx \quad (11)$$

where T_{die} and T_{solid} represents the temperature of the melt at the die exit and solidification temperature of the polymer, respectively. After integration from die temperature, T_{die}, up to freezeline temperature, T_{solid}, we can obtain equation defining the relationship between freezeline height, L, and heat transfer coefficient, HTC, which take the following simple analytical expression:

$$(12)$$

$$L = -\frac{1}{2}\dot{m} C_p \ln\left(-\frac{(T_{die}-T_{air})}{(-T_{solid}+T_{air})}\right)\frac{\varphi}{\pi HTC(\alpha pJ - \alpha BURR_0 - \sin(\varphi)R_0 - pJ\varphi + \sin(\varphi)pJ - \alpha\cos(\varphi)pJ + \alpha\cos(\varphi)BURR_0)}$$

With the aim to get equations for the temperature profile along the bubble, it is necessary to apply the Eq. 10 for any arbitrary point at the bubble i.e. in the following way:

$$\int_{T_{die}}^{T} \frac{\dot{m} C_p}{HTC(T-T_{air})} dT = 2\pi \int_{0}^{x} y dx \quad (13)$$

After the integration of Eq. 13, the temperature profile takes the following analytical expression:

$$(14)$$

$$T = T_{air} + (T_{die} - T_{air})\exp\left\{-\frac{2\pi LHTC}{\dot{m} C_p \varphi}\left(-\alpha[R_0 BUR - pJ]\left[\cos\left(\frac{x\varphi}{L}\right) - 1\right] + \sin\left(\frac{x\varphi}{L}\right)[R_0 - pJ] + pJ\varphi\frac{x}{L}\right)\right\}$$

Velocity profile calculation: With the aim to calculate the velocity profile and the film thickness in the non-isothermal film blowing process, the force balance in vertical direction (gravity and upward force due to the airflow are neglected) proposed by Pearson and Petrie is considered in the following form:

$$\frac{2\pi y h \sigma_{11}}{\sqrt{1+(y')^2}} = F - \pi \Delta p \left(R_0^2 BUR^2 - y^2\right) \quad (15)$$

where σ_{11} is the total stress in the machine direction and F and Δp are defined by Eqs. 4 in Table 1, $F_{total} = |F|$ and Eq. 5 in Table 1. The deformation rate tensor in the bubble forming region takes the following form:

$$D = \begin{pmatrix} \dot{\varepsilon}_1 & 0 & 0 \\ 0 & \dot{\varepsilon}_2 & 0 \\ 0 & 0 & \dot{\varepsilon}_3 \end{pmatrix} = \begin{pmatrix} \frac{dv}{dx} & 0 & 0 \\ 0 & \frac{v}{h}\frac{dh}{dx} & 0 \\ 0 & 0 & \frac{v}{y}y' \end{pmatrix} \quad (16)$$

where v and h is bubble velocity and thickness, respectively. Assuming that h << y, then

$$\sigma_{11} = \tau_{11} - \tau_{22} \qquad (17)$$

By combination of Eqs. 2, 16, 17, the σ_{11} takes the following form:

$$\sigma_{11} = 2\eta\left(2\frac{dv}{dx} + \frac{v}{y}y'\right) \qquad (18)$$

After substituting Eq. 18 into Eq. 15, the equation for the bubble velocity in the following form can be obtained.

$$v = v_d \, exp\left(\int_0^L \left\{\frac{\sqrt{1+(y')^2}\left[F - \pi\Delta p\left(R_0^2 BUR^2 - y^2\right)\right]}{4Q\eta} - \frac{1}{2y}y'\right\}dx\right) \qquad (19)$$

where v_d is bubble velocity at the die exit. Having the velocity profile, the deformation rates and the thickness can be properly calculated along the bubble.

Modeling versus experimental data

In this part, the above described film blowing model will be tested by using experimental data taken from the Tas's PhD thesis [18]. Moreover, theoretical predictions will be compared with two different film blowing models [15-17] (those predictions will be taken from the literature) which has already been utilized for the same experimental data set.

Material definition In this work, LDPE L8 taken from Tas's PhD thesis [18] is considered (Table 3). Material characteristics together with corresponding viscoelastic Phan-Thien-Tanner (PTT) model parameters are provided in [18]. It should be mentioned that predictions of the PTT model [41] for steady state shear and steady uniaxial extensional viscosities have been used as the measurements for LDPE L8 in order to obtain all adjustable parameters of the proposed model (Eq. 3-5), which is utilized here as the constitutive equation. This procedure has been chosen due to the fact that steady state rheological data for tested LDPE L8 is not available in Tas's PhD thesis.

In Figure 1, it is clearly visible that the used generalized Newtonian model has very good capabilities to describe steady shear and steady uniaxial extensional viscosities for the Tas's LDPE L8 sample which justifies its utilization in the film blowing modeling. The generalized Newtonian model parameters are provided in Table 4 and the parameter has been chosen to be 20 as suggested in [39].

Film blowing experiment versus model prediction In this section, proposed model predictions for the bubble shape (Figure 2), film velocity (Figure 3) and temperature profiles (Figure 4), for the processing conditions summarized in Table 4, are compared with Tas's experimental data [18] together with theoretical predictions by Sarafrazi and Sharif [16] model and Beaulne and Mitsoulis model [15] which are based on the classical approach of Pearson and Petrie [20].

It should be mentioned that two possible numerical schemes have been tested for the proposed model. First procedure consider that the bubble shape (i.e. pJ, BUR) is a priory known and take-up force F and internal bubble pressure Δp are unknowns parameters whereas in the second case, Δp is known and bubble shape (i.e. pJ, BUR) and F are unknown parameters.

As can be clearly seen in Figures 2-4, both numerical approaches leads to very similar predictions for all investigated variables (bubble shape, velocity and temperature) and it can be concluded that the agreement between the proposed model predictions are in very good agreement with the corresponding experimental data. Moreover, tested model predictions are comparable with the Sarafrazi/Sharif [16] model predictions (which is based on the advanced eXtended Pom-Pom constitutive equation; a variable heat transfer coefficient and stress induced crystallization).

Complete set of calculated variables in the proposed model for theoretical predictions depicted in Figures 2-4 are summarized in Table 5. It is nicely visible that predicted F and Δp for all tested polymers and processing conditions are in fairly good agreement with the corresponding Tas's experimental data. These predictions are comparable with Sarafrazi/Sharif [16] model predictions and even better than Beaulne and Mitsoulis model [15] behavior which is based on the viscoelastic integral constitutive equation of the K-BKZ type assuming constant heat transfer coefficient and no crystallization effects. Just note that for the die volume rate calculation (from the experimentally known mass flow rate), the following definition of the LDPE density taken from [18] was used:

$$\rho = \frac{1000}{0.934 \cdot 0.001 \cdot (273.15 + T_{die}) + 0.875} \qquad (20)$$

Conclusion

It has been shown that minimum energy approach (considering non-isothermal processing conditions and recently proposed generalized Newtonian model) can be taken as the useful modeling tool for the film blowing process due to its qualitative as well as qualitative prediction capabilities in terms of internal bubble pressure, take-up force, bubble shape, velocity and temperature profiles.

Acknowledgments

References

1. S. Kim, Y.L. Fang, P. G. Lafleur and P. J. Carreau, Polym. Eng. Sci. 44, 283-302 (2004).
2. R. S. Mayavaram, "Modeling and simulation of film blowing process", Ph.D. Thesis, A&M University Texas, 2005.
3. K. Cantor, Blown Film Extrusion, Munich: Cark Hanser Verlag, 2006, p. 165.
4. C. D. Han and J. Y. Park, J. Appl. Polym. Sci. 19, 3277 (1975).
5. C. D. Han and J. Y. Park, J. Appl. Polymer Sci. 19, 3291 (1975).
6. Y. L. Yeow, J. Fluid Mech 75, 577-591 (1976).
7. C. D. Han and R. Shetty, Ind. Eng. Chem. Fund. 16, 49 (1977).
8. T. Kanai and J. L. White, Polym. Eng. Sci. 24, 1185 (1984).
9. W. Minoshima and J. L. White, J. Non-Newtonian Fluid Mech. 19, 275 (1986).
10. T. Kanai and J. L. White, J. Non-Newtonian Fluid Mech. 19, 275 (1986).
11. T. J. Obijeski and K. R. Puritt, SPE ANTEC Tech. Papers 1, 150 (1992).
12. P. A. Sweeney and G. A. Campbell, SPE ANTEC Tech. Papers 461, 461 (1993).
13. T. Kanai and G. A. Campbell, Film Processing: Progress in Polymer Processing, Munich: Hanser Gardner Publications, 1999.
14. T. I. Butler, SPE ANTEC Tech. Papers 1, 1120 (2000).
15. M. Beaulne and E. Mitsoulis, J. Appl. Polym. Sci. 105, 2098-2112 (2007).
16. S. Sarafrazi and F. Sharif, International Polymer Processing. 23, 30-37 (2008).
17. I. A. Muslet and M. R. Kamal, J. Rheol. 48, 525-550 (2004).
18. P. P. Tas, "Film blowing from polymer to product", Ph.D. Thesis, Technische Universitat Eindhoven, 1994.
19. R. K. Gupta, "A new non-isothermal rheological constitutive equation and its application to industrial film blowing", Ph.D. Thesis, University of Delaware, 1981.
20. J. R. A. Pearson and C.J.S. Petrie, J. Fluid. Mech. 40, 1 (1970).
21. J. R. A. Pearson and C.J.S. Petrie, J. Fluid. Mech. 42, 609 (1970).
22. J. R. A. Pearson and C.J.S. Petrie, Plast. Polym. 38, 85 (1970).
23. C. J. S. Petrie, "Film blowing, blow moulding and thermoforming," in Applied Science, edited by J. R. A. Pearson and S.M. Richardson, London, 1983, p. 217.
24. C. D. Han and J. Y. Park, J. Appl. Polym. Sci. 19, 3277 (1975).
25. C. J. S. Petrie, Am. Inst. Chem. Eng. J. 21, 275 (1975).
26. X. L. Luo and R. I. Tanner, Polym. Eng. Sci. 25, 620 (1985).
27. B. K. Ashok and G. A. Campbell, Int. Polym. Proc. 7, 240 (1992).
28. S. M. Alaie and T. C. Papanastasiou, Int. Polym. Proc. 8, 51 (1993).
29. J. M. Andr´e, Y. Demay, J. M. Haudin, B. Monasse and J. F. Agassant, Int. J. Form. Proc. 1, 187 (1998).
30. M. Zatloukal, J. Non-Newtonian Fluid Mech. 113, 209 (2003).
31. M. Zatloukal and J. Vlcek, J. Non-Newtonian Fluid Mech. 123, 201-213 (2004).
32. M. Zatloukal, J. Vlcek, P. Saha, Annual Technical Conference - ANTEC, Conference Proceedings 1, 235-239 (2004).
33. M. Zatloukal and J. Vlcek, Annual Technical Conference - ANTEC, Conference Proceedings 1, 139-142 (2005).
34. M. Zatloukal and J. Vlcek, J. Non-Newtonian Fluid Mech. 133, 63-72 (2006).
35. M. Zatloukal, H. Mavridis, J. Vlcek and P. Saha, Annual Technical Conference - ANTEC, Conference Proceedings 2, 825-829 (2006).
36. M. Zatloukal, H. Mavridis, J. Vlcek and P. Saha, Annual Technical Conference - ANTEC, Conference Proceedings 3, 1579-1583 (2007).
37. C. C. Liu, D. C. Bogue, J. E. Spruiell, Int. Polym. Process. 10, 226 (1995).
38. C. C. Liu, D. C. Bogue, J. E. Spruiell, Int. Polym. Process. 10, 230 (1995).
39. M. Zatloukal, J. Non-Newtonian Fluid Mech. 165 (2010) 592-595.
40. A. K Doufas and A.J. McHugh, J. Rheol. 45, 1085 (2001).
41. N. Phan-Thien, R. I. Tanner, J. Non-Newtonian Fluid Mech. 2 (1977) 353–365.

Equation type	Equation form	Equation number
Bubble shape	$y = (R_0 - pJ)\cos\left(\dfrac{x\varphi}{L}\right) - \alpha'(pJ - BURR_0)\sin\left(\dfrac{x\varphi}{L}\right) + pJ$	(1)
α' function	$\alpha' = \sqrt{\dfrac{2pJ - R_0 - BURR_0}{pJ - BURR_0}\left\| \dfrac{R_0(BUR - 1)}{pJ - BURR_0}\right\|}$	(2)
A function	$A = \dfrac{pJ - R_0}{pJ - BURR_0}$	(3)
Take-up force	$F = -\dfrac{L^2}{J\varphi^2}$	(4)
Internal bubble pressure	$\Delta p = \dfrac{pL}{2\pi \int\limits_0^L y\sqrt{1 + (y')^2}\,dx}$	(5)

TABLE 1. A Summary of the Zatloukal-Vlcek mode

Equation	A	φ
1.	1	0
2.	$0 < A < 1$	$arctg\left(\dfrac{\sqrt{1 - A^2}}{A}\right)$
3.	0	$\pi/2$
4.	$-1 < A < 0$	$\pi + arctg\left(\dfrac{\sqrt{1 - A^2}}{A}\right)$
5.	-1	π

TABLE 2. Relationship between A and phi functions.

LDPE material	Grade (Stamylan LD)	Melt Index (dg·min⁻¹)	M_n (g·mol⁻¹)	M_w (g·mol⁻¹)	M_z (g·mol⁻¹)	Density (kg·m⁻³)	Crystallization temperature T_c (°C)
			Molecular weight averages				
L8	2008XC43	8	13000	155000	780000	920	98.6

TABLE. 3. Characteristics of the L8 Stamylan LDPE used in the experiments by T as [18].

L8 Exp.	BUR (-)	L (m)	pJ (m)	Δp (Pa)	R_0 (m)	H_0 (m)	TUR (-)	$\dot{m}$ (kg·h⁻¹)
	Parameters of the generalized Newtonian constitutive equation							
29	2.749	0.13882	0.029818	70	0.0178	0.0022	19.4437	0.00100

η_0 (Pa·s)	λ (s)	a (-)	n (-)	α (s)	β (-)	ζ (-)
Parameters of the generalized Newtonian constitutive equation ($\psi=20$)						
2365	0.17242	0.71597	0.37108	$1\cdot10^{-5}$	$9.21\cdot10^{-7}$	0.054384

T_{air} (°C)	T_{solid} (°C)	T_{die} (°C)	T_r (°C)	E_a (J·mol⁻¹)	R (J·K⁻¹·mol⁻¹)	C_p (J·kg⁻¹·K⁻¹)
Temperature parameters						
25	92	145	190	59000	8.314	2300

TABLE 4. Film blowing model parameters for Tas's experiments No. 29.

Models	Experiment 29			
L8	Δp (Pa)	F (N)	σ_{11} (MPa)	σ_{33} (MPa)
Experimental data (Tas)	70	3.5	0.270	0.070
Zatloukal-Vlcek	70.000 (46.341)	5.724 (5.619)	0.452 (0.444)	0.083 (0.055)
Sarafrazi and Sharif	55.84	3.34	0.3110	0.0375
Beaulne and Mitsoulis	168	2.13	0.206*	0.245*

TABLE 5. Summarization of Tas's experimental data [18], Zatloukal-Vlcek [39] (the calculated results for the fixed bubble shape pJ and internal bubble pressure (delta)p are provided in the brackets and without brackets, respectively), Sarafrazi/Sharif [16] and Beaulne/Mitsoulis [15] model predictions for Tas's LDPEs and processing conditions.

Petrie equations $\sigma_{11} = \dfrac{F}{2\pi R_0 BURH_1}$ and $\sigma_{33} = \dfrac{R_0 BUR\Delta p}{H_1}$

- σ_{11}, σ_{33} at the freezeline were calculated by using v_d, R_0, H_0, F, Δp, BUR, v_f provided in [15] and Pearson and

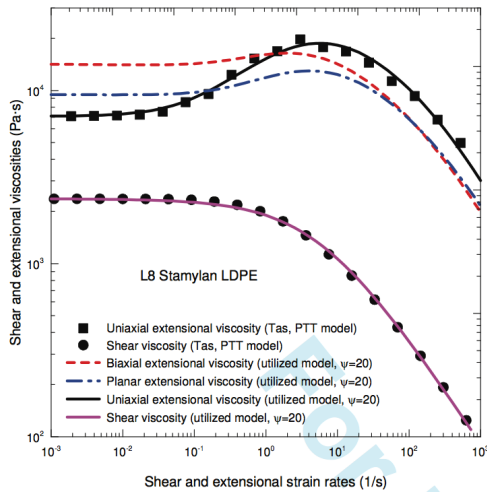
FIGURE 1. Comparison between the generalized Newtonian model fit (solid lines) [39] and PTT model predictions (symbols) characterizing L8 Stamylan LDPE material according to Tas's Ph.D. thesis [18].

FIGURE 2. Comparison of the bubble shapes between the proposed model prediction [30], experiment No. 29 taken from Tas´s Ph.D. thesis [18] and the Beaulne/Mitsoulis model prediction [15] and the Sarafrazi/Sharif model prediction [16].
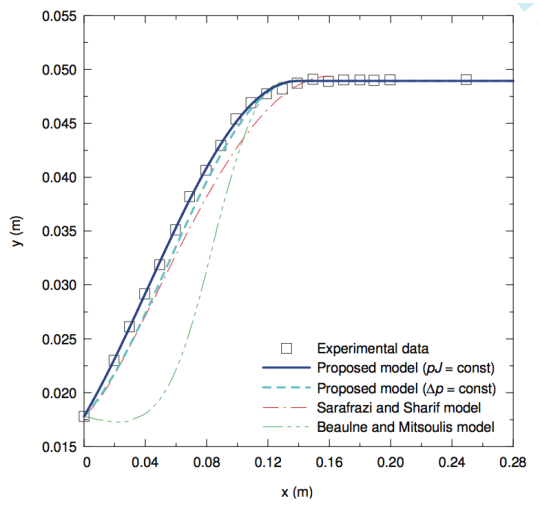
FIGURE 3. Comparison of the velocity profiles between the proposed model prediction [30], experiment No. 29 taken from Tas's Ph.D. thesis [18] and the Beaulne/Mitsoulis model prediction [15] and the Sarafrazi/Sharif model prediction [16].
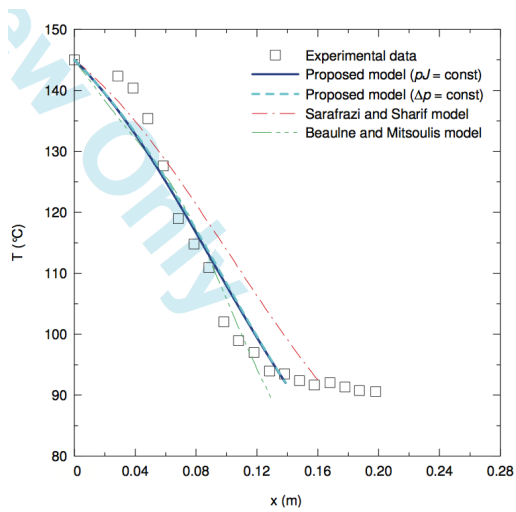

FIGURE 4. Comparison of the temperature profiles between the proposed model prediction [30], experiment No. 29 taken from Tas's Ph.D. thesis [18] and the Beaulne/Mitsoulis model prediction [15] and the Sarafrazi/Sharif model prediction [16].

Return to Paper of the Month.